nature geoscience

ARTICLES

PUBLISHED ONLINE: 25 APRIL 2017 | DOI: 10.1038/NGEO2943

Global aquifers dominated by fossil groundwaters but wells vulnerable to modern contamination

Scott Jasechko[1]*, Debra Perrone[2,3], Kevin M. Befus[4], M. Bayani Cardenas[5], Grant Ferguson[6], Tom Gleeson[7], Elco Luijendijk[8], Jeffrey J. McDonnell[9,10,11], Richard G. Taylor[12], Yoshihide Wada[13,14] and James W. Kirchner[15,16,17]

The vulnerability of groundwater to contamination is closely related to its age. Groundwaters that infiltrated prior to the Holocene have been documented in many aquifers and are widely assumed to be unaffected by modern contamination. However, the global prevalence of these 'fossil' groundwaters and their vulnerability to modern-era pollutants remain unclear. Here we analyse groundwater carbon isotope data (^{12}C, ^{13}C, ^{14}C) from 6,455 wells around the globe. We show that fossil groundwaters comprise a large share (42–85%) of total aquifer storage in the upper 1 km of the crust, and the majority of waters pumped from wells deeper than 250 m. However, half of the wells in our study that are dominated by fossil groundwater also contain detectable levels of tritium, indicating the presence of much younger, decadal-age waters and suggesting that contemporary contaminants may be able to reach deep wells that tap fossil aquifers. We conclude that water quality risk should be considered along with sustainable use when managing fossil groundwater resources.

Global groundwater is an immense resource, storing ~100 times more water than all the world's lakes[1,2], supplying ~40% of the water for global irrigated agriculture[3], and providing drinking water to billions of people around the world. Recent research has evaluated the global depths of both the groundwater table[4] and modern groundwater recharged within the past ~50 years[1], but the global prevalence and distribution of 'fossil groundwater' remain unclear. Here we define fossil groundwater as groundwater recharged by precipitation more than ~12,000 years ago, prior to the beginning of the Holocene epoch; we define prevalence as the frequency with which regional well waters contain fossil groundwater. Understanding the global extent and depth of fossil groundwater resources is important because of their distinctive susceptibility to overdraft[5], presumed isolation from surface-borne pollutants[6,7], potential vulnerability to geogenic contaminants[8], and isolation from modern climate variability[9].

To calculate the prevalence of fossil groundwater in well waters, we compiled a groundwater carbon isotope (^{12}C, ^{13}C, ^{14}C) database of 6,455 well water samples from around the globe. The continental USA and Europe are over-represented in our compilation, which is also inevitably biased towards sedimentary basins where groundwater use is common (Supplementary Figs 1,2 and Methods). Radiocarbon (^{14}C) has a half-life of 5,730 years and has been widely used to identify fossil groundwaters[10–18]. Stable carbon isotope (^{12}C, ^{13}C) data were used to correct for the dissolution of carbonate rocks, which are devoid of radiocarbon[19] and thus would otherwise distort ^{14}C-based fossil groundwater calculations. We estimated fossil groundwater fractions in wells around the world using a recently developed radiocarbon endmember mixing model, which accounts for both radioactive decay and carbonate dissolution for pre- and post-Holocene recharge[20]. Our approach, which estimates the fraction of fossil groundwater in a water sample rather than the sample's average age, is designed to be less vulnerable to the aggregation errors that are known to bias mean groundwater age calculations[21–23]. We plotted depth profiles of fossil groundwater for aquifers around the world and calculated the depth below which fossil groundwater becomes common (>50% of wells pump some fossil groundwater) or dominant (>50% of wells pump >50% fossil groundwater; Methods). Where tritium (^{3}H) data were available ($n = 5{,}661$ well water samples), we determined the fraction of the groundwater sample that recharged more recently than around 1953 by relating groundwater ^{3}H concentrations to historical precipitation ^{3}H time series[24] (Methods). The threshold year 1953 was selected because widespread thermonuclear testing in subsequent years increased precipitation tritium levels by ~5 to ~500 times above local natural background concentrations[24], providing a tracer of recently recharged groundwater (for example, ref. 15). For samples with both radiocarbon and tritium data, we

[1]Department of Geography, University of Calgary, Calgary, Alberta T2N 4H7, Canada. [2]Water in the West, Stanford University, Stanford, California 94305, USA. [3]Civil and Environmental Engineering, Stanford University, Stanford, California 94305, USA. [4]Civil and Architectural Engineering, University of Wyoming, Laramie, Wyoming 82071, USA. [5]Department of Geological Sciences, The University of Texas at Austin, Austin, Texas 78712, USA. [6]Department of Civil and Geological Engineering, University of Saskatchewan, Saskatoon, Saskatchewan S7N 5A9, Canada. [7]Department of Civil Engineering and School of Earth and Ocean Sciences, University of Victoria, Victoria, British Columbia V8P 5C2, Canada. [8]Geoscience Centre, University of Göttingen, Göttingen 37077, Germany. [9]Global Institute for Water Security, and School of Environment and Sustainability, University of Saskatchewan, Saskatoon, Saskatchewan S7N 3H5, Canada. [10]School of Geosciences, University of Aberdeen, Aberdeen AB24 3FX, UK. [11]Department for Forest Engineering, Resources and Management, Oregon State University, Corvallis, Oregon 97330, USA. [12]Department of Geography, University College London, London WC1E 6BT, UK. [13]International Institute for Applied Systems Analysis, Schlossplatz 1, Laxenburg A-2361, Austria. [14]Department of Physical Geography, Utrecht University, Utrecht 80115, The Netherlands. [15]Department of Environmental System Sciences, ETH Zürich, Universitätstrasse 16, CH-8092, Switzerland. [16]Swiss Federal Research Institute WSL, Birmensdorf CH-8903, Switzerland. [17]Department of Earth and Planetary Science, University of California, Berkeley, California 94720, USA. *e-mail: sjasechk@ucalgary.ca

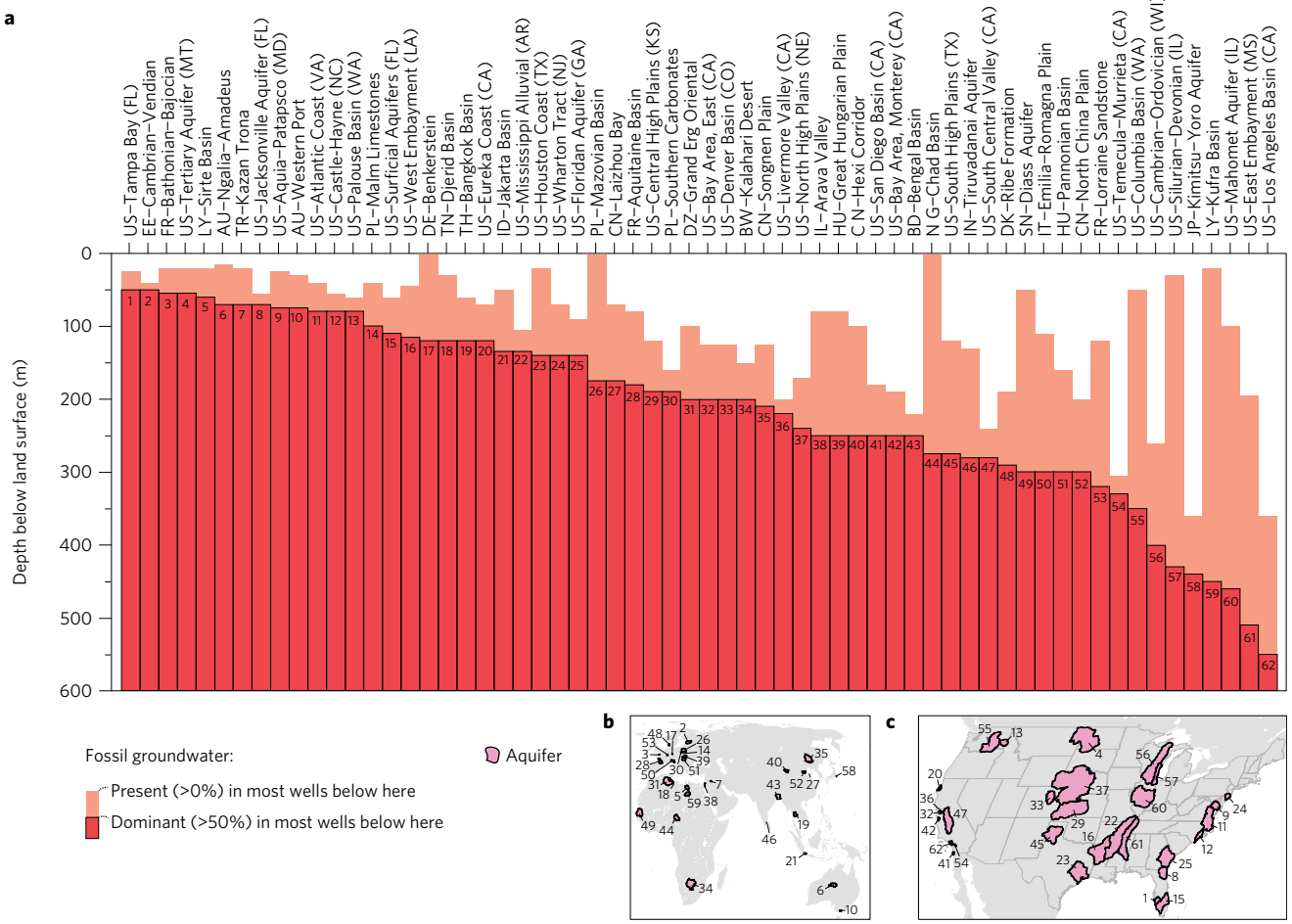

Figure 1 | Prevalence of fossil groundwater in global aquifers. a, Depth to the fossil groundwater transition in 62 aquifers. The shallow depth (top of peach bar) represents a depth below which most wells (>50%) contain detectable fossil groundwater (minimum fossil groundwater fraction >0%). The deeper depth (top of red bar) represents a depth below which most wells (>50%) are dominated by fossil groundwater (minimum fossil groundwater fraction is >50%). Fossil groundwater becomes dominant at a median depth of 200 m (lower–upper quartiles are 115–290 m). The lower limit of our graph (600 m) does not necessarily represent the lower boundary for our study aquifers, nor do the depths covered by red and orange bars imply that groundwater is of high quality. **b**,**c**, Locations of the 62 aquifers.

calculated the three fractions of groundwater that recharged more than ~12 thousand years ago (fossil groundwater); recharged more recently than the year 1953 (post-1953 groundwater); and is of an intermediate age, having recharged more recently than ~12 thousand years ago, but before the year 1953.

Fossil groundwater in global aquifers

Our global compilation of radiocarbon data shows that fossil groundwater is not an anomaly in the upper 1 km of the crust, but instead is common in wells drilled to depths of more than ~250 m (Figs 1, 2 and Supplementary Fig. 3). Among all surveyed wells ($n = 6{,}455$; Supplementary Fig. 3), we find that more than half of all wells deeper than 250 m yield groundwater that was mostly (>50%) replenished before the Holocene (that is, minimum fossil groundwater exceeds 50% for the majority of groundwater samples pumped from wells deeper than 250 m). By contrast, post-1953 groundwater becomes increasingly scarce with depth (Fig. 2). Half of all wells deeper than 40 m pump groundwater that is comprised almost entirely (>90%) of groundwater recharged before 1953 (that is, maximum post-1953 groundwater is less than 10% for the majority of groundwater samples pumped from deeper than 40 m).

Fossil groundwaters are found throughout several major aquifers that sustain modern irrigated agriculture (Fig. 1), including the North China Plain (at depths >200 m), the southern Central Valley of California (at depths >260 m), the north, central and south High Plains aquifers of the central USA (at depths >120–280 m), Italy's Emilia–Romagna Plain (at depths >100–300 m) and Hungary's Pannonian Basin (at depths >160–300 m). Among our 62 study aquifers (Fig. 1), we find the range of depths below which fossil groundwaters dominate well waters (that is, fossil groundwaters comprise >50% of the water pumped from more than half of all deeper samples) has a median of 200 m, a lower–upper quartile range of 115–290 m, and a 10th–90th percentile range of 70–430 m.

Assuming that isotopes measured in well waters reflect the isotope compositions of groundwater stored in aquifers and are not the result of contamination by infiltrated surface water or rainfall (for example, refs 1,5,11–18), our data show that fossil groundwater likely comprises 42–85% of total groundwater in the crust's uppermost 1 km, 31–79% in the uppermost 500 m, and 10–63% in the uppermost 100 m (Fig. 2c). By contrast, post-1953 groundwater comprises only 5–22% of total groundwater in the crust's uppermost 1 km, 6–27% in the uppermost 500 m, and 13–51% in the uppermost 100 m (Fig. 2d). Fossil groundwater storage in the uppermost 1 km of the crust is, therefore, ~1.9 to ~17 times larger than post-1953 groundwater stores. By combining our new global fossil groundwater storage estimate with global porosity data[1], we calculate that of the 12–22 million km^3 of unfrozen water stored

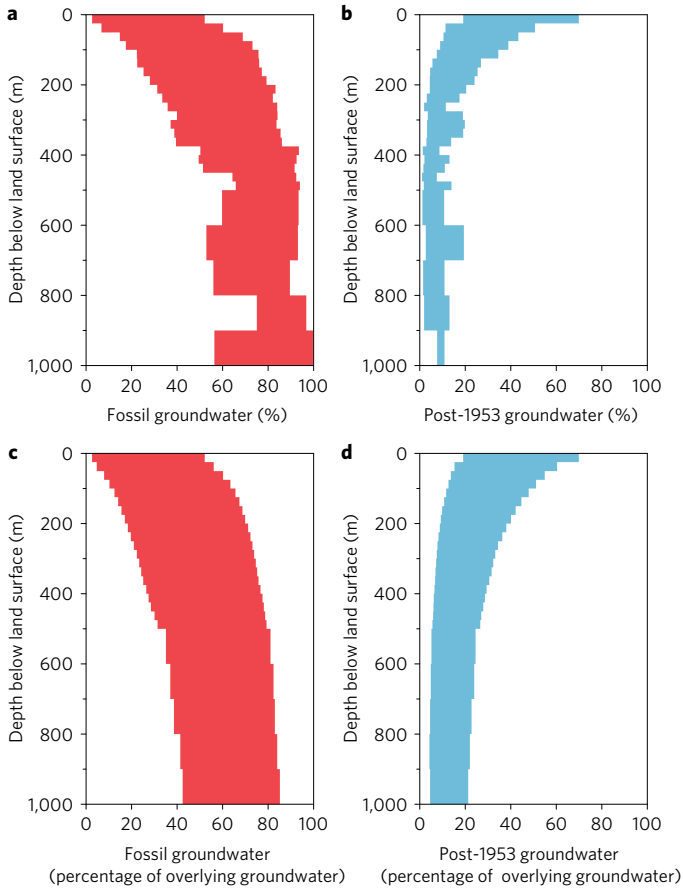

Figure 2 | Variations of fossil and post-1953 groundwater with depth. **a**,**b**, Statistical distributions of fossil (red) and post-1953 (blue) groundwater, respectively, binned at various depths. **c**,**d**, Cumulative distribution with depth of stored fossil groundwater and post-1953 groundwater, respectively; that is, these panels represent the fraction of total groundwater overlying a given depth (corrected for porosity changes with depth; ref. 1). Coloured areas represent estimated maximum and minimum ranges, calculated using all groundwater samples within a given depth bin (average of maximum and minimum fossil and post-1953 groundwater estimates for a given range of well depths).

in the uppermost 1 km of the crust[1] (~85–152 m equivalent depth of a column of water), approximately 5–18 million km^3 is fossil groundwater (36–130 m equivalent depth), 0.6–4.6 million km^3 is post-1953 groundwater (4–33 m equivalent depth), and less than 8,000 km^3 is recent rain and snow that becomes streamflow in less than three months[25] (<0.055 m equivalent depth).

Figures 1 and 2 show that the abundance of modern (post-1953) groundwater generally decreases with depth and that the abundance of fossil groundwater generally increases with depth. Topography-driven groundwater flow, geologic layering, and the decrease of permeability with depth generally lead to well-flushed shallow zones overlying poorly flushed deeper zones, consistent with the occurrence of fossil groundwaters at depth. We conclude that a substantial share (42–85%) of global groundwater in the upper 1 km of the crust is fossil in age. Further, our analysis may even underestimate fossil groundwater abundance because of possible sampling biases towards more permeable basins, contamination of samples by atmospheric $^{14}CO_2$ that would bias our results to smaller fossil groundwater fractions[26], preferential pumping from more permeable strata that may be more likely to contain younger groundwaters (Supplementary Section 3), and contamination of well waters by recent precipitation due to the construction and use of the well itself (see subsequent section). Although our finding that old water is more common at greater depths is highly intuitive, our analysis is the first global, empirical assessment of the depths at which global aquifer systems transition to poorly flushed storage dominated by fossil groundwaters.

Global groundwater use is accelerating[27,28]. Declining water tables, more intense droughts, and improved well construction technologies may encourage deeper drilling and increase society's reliance on fossil groundwaters. Assessing how much fossil groundwater is pumped from aquifers requires records of well construction depths, which are available in the western US (Supplementary Section 4) but not available globally. We examined how frequently fossil groundwaters are pumped in three western US groundwater aquifers by relating constructed well depths to ^{14}C-based fossil groundwater abundances (Supplementary Section 4). In the northern High Plains, 99% of wells are shallower than the depth below which fossil groundwaters become common (~170 m), implying that fossil groundwater pumping here is relatively rare (Supplementary Fig. 6). Similarly, in the San Joaquin Valley, the large majority (98%) of wells are shallower than the depth below which fossil groundwater becomes common (~240 m). In the Denver Basin, however, many (38%) groundwater wells have been constructed to depths where fossil groundwater is either detectable or dominant (>125 m), implying that fossil groundwater use in the Denver Basin is widespread (Supplementary Fig. 6). Further, fossil groundwater pumping in the Denver Basin has probably increased over the past ~60 years because older wells drilled between 1950 and 1970 were substantially shallower (median well depth of 27 m) than wells constructed more recently than 2010 (median well depth of 126 m), and because total groundwater pumping has more than quadrupled since 1970 (ref. 29).

Our comparison of groundwater well depths and vertical distributions of fossil groundwater emphasizes that both fossil and post-1953 groundwaters are withdrawn from US aquifers. Pumping fossil groundwater may lead to aquifer depletion, and this risk is greater in arid regions where groundwater tables are deeper and compensatory increases in recharge or decreases in groundwater discharge are less likely (see ref. 30). Water levels in deep wells have declined across much of the US over the past six decades, probably due to changes in groundwater pumping in response to climate variations[31]. Groundwater well construction is guided by aquifer properties (for example, transmissivity) and groundwater quality (for example, salinity) rather than groundwater age. Nevertheless, we conclude that deep fossil groundwater is already used in some parts of the US, and posit that reliance on fossil groundwaters is probably also widespread in other regions, particularly in hyper-arid climates where modern recharge is negligible.

Fossil well waters vulnerable to contamination

Our compilation of radiocarbon and tritium data shows that roughly half of the well water samples that are measurably depleted in carbonate-dissolution-corrected ^{14}C (which is clear evidence of fossil age) also contain measurable amounts of ^{3}H (which is unequivocal evidence of recharge after the onset of thermonuclear-bomb testing in the 1950s; Table 1). This observation questions the common perception that fossil groundwaters are largely immune to modern contamination (for example, refs 6,7). Our finding that fossil well waters often contain a component of much younger, decades-old groundwater means that fossil well waters—and, possibly, the aquifers from which they derive—are more vulnerable to pollution from modern-era contaminants than previously thought.

Several processes can mix decadal-age groundwater with fossil groundwater and thus make fossil well waters vulnerable to modern contaminants. One plausible explanation is aquifer heterogeneity, leading to preferential flow of younger groundwater through

Table 1 | Radioisotope (^{14}C, ^{3}H) evidence for post-1953 and fossil groundwater mixing.

Presence of fossil groundwater	Total ^{14}C samples with ^{3}H data	Presence of post-1953 groundwater	
		Present ($^{3}H > 0$)	Absent ($^{3}H \approx 0$)
May contain no fossil water (possibly 0%)	$n = 984$	74%	26%
Contains fossil water (>0%), but possibly <50%	$n = 179$	49%	51%
Contains mostly fossil water (>50%)	$n = 365$	50%	50%

high-permeability zones and slower flows of correspondingly older groundwater through less permeable parts of the aquifer system, with mixing of these different-aged waters by dispersion or diffusion. Topography-driven multi-scale groundwater flow can also result in adjacent groundwater flow paths with very different ages, and thus there can be substantial mixing or dispersion of ages where flow paths converge, such as low-lying discharge areas on the land surface[32,33]. Induced mixing of young and old waters could also occur in wells with open holes or long screens that simultaneously capture young and old groundwater from shallow and deep layers of an aquifer[34,35]. Leaks in corroded or poorly sealed portions of a well may also contribute to mixing of young and old waters in the well bore itself. Co-occurrences of fossil and post-1953 groundwater pumped from wells perforated hundreds of metres below the land surface more likely arise from the construction, presence and use of the well itself. For some hydrogeologic settings, it is unlikely that natural flow paths transmit groundwater hundreds of metres below the land surface within a few decades. We note that tritium occurs equally often in well waters containing some fossil groundwater (tritium was detected in approximately half of all samples with >0%) and in well waters containing mostly fossil groundwater (tritium was also detected in approximately half of samples with >50% fossil water). If natural flow paths were the primary cause of the widespread mixing of fossil and post-1953 groundwater, we would expect that samples dominated by fossil groundwater (>50%) would contain measurable tritium less frequently than samples that contain some fossil groundwater (>0% but possibly <50% fossil water), which is not the case (Table 1). Thus, tritium may co-occur with fossil groundwaters primarily as a result of pumping along extensive well screens, up-coning and down-coning of groundwater due to pumping, and leaks along well bores.

Regardless of how tritium has become mixed with much older groundwaters, the main implication for drinking water supplies is clear: many (~50%) fossil well waters contain detectable amounts of recently recharged groundwater (Table 1), rendering them potentially vulnerable to modern anthropogenic contamination despite their great age. Because aquifers bearing fossil groundwater require millennia to be flushed, their contamination may also persist for millennia, causing effectively irreversible harm to these aquifers over human timescales. However, it remains unclear how frequently tritium arises in fossil well waters as the result of mixing within the aquifer itself, versus mixing induced by the construction and pumping of the groundwater well.

Fossil groundwater resources

Our analysis shows that fossil groundwater probably dominates global groundwater storage in the uppermost 1 km of the crust (42–85%). This figure is likely to be a lower bound on the global prevalence of fossil groundwater, because the probable biases in our analysis (detailed above) serve to minimize our calculated fossil groundwater fractions. Further, our analysis focuses solely on the shallowest 1 km of the crust that is also the most rapidly flushed. Fractured rocks deeper than 1 km can host ancient fossil groundwaters that have been isolated for millions or even billions of years[36,37].

Improving access to freshwater for agriculture, households, and industry while sustaining vital ecosystems in a changing global environment represents a critical scientific and political challenge. Fossil groundwater resources probably comprise more than half of global unfrozen freshwater (Figs 1 and 2), and dependence upon fossil groundwater to meet water demands is rising as a consequence of increasing groundwater withdrawals and deeper drilling in some regions. Groundwater quality remains a critical concern in many parts of the world[38–41], and our results highlight that even though deeper wells pump predominantly fossil groundwater, they are not immune to modern contamination.

Methods

Methods, including statements of data availability and any associated accession codes and references, are available in the online version of this paper.

Received 31 October 2016; accepted 29 March 2017; published online 25 April 2017

References

1. Gleeson, T., Befus, K. M., Jasechko, S., Luijendijk, E. & Cardenas, M. B. The global volume and distribution of modern groundwater. *Nat. Geosci.* **9,** 161–168 (2016).
2. Messager, M. L., Lehner, B., Grill, G., Nedeva, I. & Schmitt, O. Estimating the volume and age of water stored in global lakes using a geo-statistical approach. *Nat. Commun.* **7,** 13603 (2016).
3. Siebert, S. *et al*. Groundwater use for irrigation—a global inventory. *Hydrol. Earth Syst. Sci.* **14,** 1863–1880 (2010).
4. Fan, Y., Li, H. & Miguez-Macho, G. Global patterns of groundwater table depth. *Science* **339,** 940–943 (2013).
5. Chen, Z., Nie, Z., Zhang, Z., Qi, J. & Nan, Y. Isotopes and sustainability of ground water resources, North China Plain. *Groundwater* **43,** 485–493 (2005).
6. Yamada, C. *First Report on Shared Natural Resources* (United Nations International Law Commission, A/CN.4/533 + Add.1, 2003); http://www.legal.un.org/ilc/documentation/english/a_cn4_533.pdf
7. Buser, H. R. Atrazine and other s-triazine herbicides in lakes and in rain in Switzerland. *Environ. Sci. Technol.* **24,** 1049–1058 (1990).
8. Burgess, W. G. *et al*. Vulnerability of deep groundwater in the Bengal Aquifer System to contamination by arsenic. *Nat. Geosci.* **3,** 83–87 (2010).
9. Taylor, R. G. *et al*. Ground water and climate change. *Nat. Clim. Change* **3,** 322–329 (2013).
10. Thatcher, L., Rubin, M. & Brown, G. F. Dating desert groundwater. *Science* **134,** 105–106 (1961).
11. Edmunds, W. M. & Wright, E. P. Groundwater recharge and palaeoclimate in the Sirte and Kufra basins, Libya. *J. Hydrol.* **40,** 215–241 (1979).
12. Phillips, F. M., Peeters, L. A., Tansey, M. K. & Davis, S. N. Paleoclimatic inferences from an isotopic investigation of groundwater in the central San Juan Basin, New Mexico. *Quat. Res.* **26,** 179–193 (1986).
13. Weyhenmeyer, C. E. *et al*. Cool glacial temperatures and changes in moisture source recorded in Oman groundwaters. *Science* **287,** 842–845 (2000).
14. Plummer, N. L. & Sprinkle, C. L. Radiocarbon dating of dissolved inorganic carbon in groundwater from confined parts of the Upper Floridan aquifer, Florida, USA. *Hydrogeol. J.* **9,** 127–150 (2001).
15. Vengosh, A., Gill, J., Davisson, M. L. & Hudson, G. B. A multi-isotope (B, Sr, O, H, and C) and age dating (^{3}H–^{3}He, and ^{14}C) study of groundwater from Salinas Valley, California: hydrochemistry, dynamics, and contamination processes. *Wat. Resour. Res.* **38,** 1008 (2002).
16. Brown, K. B., McIntosh, J. C., Baker, V. R. & Gosch, D. Isotopically-depleted late Pleistocene groundwater in Columbia River Basalt aquifers: evidence for recharge of glacial Lake Missoula floodwaters? *Geophys. Res. Lett.* **37,** L21402 (2010).
17. Morrissey, S. K., Clark, J. F., Bennett, M., Richardson, E. & Stute, M. Groundwater reorganization in the Floridan aquifer following Holocene sea-level rise. *Nat. Geosci.* **3,** 683–687 (2010).

18. Cartwright, I. & Weaver, T. R. Hydrogeochemistry of the Goulburn Valley region of the Murray Basin, Australia: implications for flow paths and resource vulnerability. *Hydrogeol. J.* **13,** 752–770 (2005).
19. Vogel, J. C. *Isotope Hydrology* 225–239 (International Atomic Energy Agency STI/PUB/255, 1970).
20. Jasechko, S. Partitioning young and old groundwater with geochemical tracers. *Chem. Geol.* **427,** 35–42 (2016).
21. Weissmann, G. S., Zhang, Y., LaBolle, E. M. & Fogg, G. E. Dispersion of groundwater age in an alluvial aquifer system. *Wat. Resour. Res.* **38,** 1198 (2002).
22. Bethke, C. M. & andJohnson, T. M. Groundwater age and groundwater age dating. *Annu. Rev. Earth Planet. Sci.* **36,** 121–152 (2008).
23. Torgersen, T. *et al*. *Isotope Methods for Dating Old Groundwater* (International Atomic Energy Agency, 2013).
24. Jasechko, S. & Taylor, R. G. Intensive rainfall recharges tropical groundwaters. *Environ. Res. Lett.* **10,** 124015 (2015).
25. Jasechko, S., Kirchner, J. W., Welker, J. M. & McDonnell, J. J. Substantial proportion of global streamflow less than three months old. *Nat. Geosci.* **9,** 126–129 (2016).
26. Aggarwal, P. K., Araguas-Araguas, L., Choudhry, M., van Duren, M. & Froehlich, K. Lower groundwater ^{14}C age by atmospheric CO_2 uptake during sampling and analysis. *Groundwater* **52,** 20–24 (2014).
27. Wada, Y., Wisser, D. & Bierkens, M. F. P. Global modeling of withdrawal, allocation and consumptive use of surface water and groundwater resources. *Earth Syst. Dyn.* **5,** 15–40 (2014).
28. Famiglietti, J. S. The global groundwater crisis. *Nat. Clim. Change* **4,** 945–948 (2014).
29. Bauch, N. J., Musgrove, M., Mahler, B. J. & Paschke, S. S. *The quality of our Nation's waters—Water Quality in the Denver Basin Aquifer System, Colorado, 2003-05* U.S. Geological Survey Circular 1357 (2014).
30. Theis, C. V. The source of water derived from wells. *Civil Eng.* **10,** 277–280 (1940).
31. Russo, T. A. & Lall, U. Depletion and response of deep groundwater to climate-induced pumping variability. *Nat. Geosci.* **10,** 105–108 (2017).
32. Toth, J. A theoretical analysis of groundwater flow in small drainage basins. *J. Geophys. Res.* **68,** 4795–4812 (1963).
33. Jiang, X. W., Wan, L., Cardenas, M. B., Ge, S. & Wang, X. S. Simultaneous rejuvenation and aging of groundwater in basins due to depth-decaying hydraulic conductivity and porosity. *Geophys. Res. Lett.* **37,** L05403 (2010).
34. Zinn, B. A. & Konikow, L. F. Effects of intraborehole flow on groundwater age distribution. *Hydrogeol. J.* **15,** 633–643 (2007).
35. Ferguson, G. A., Betcher, R. N. & Grasby, S. E. Hydrogeology of the Winnipeg formation in Manitoba, Canada. *Hydrogeol. J.* **15,** 573–587 (2007).
36. Lin, L. H. *et al*. Long-term sustainability of a high-energy, low-diversity crustal biome. *Science* **314,** 479–482 (2006).
37. Holland, G. *et al*. Deep fracture fluids isolated in the crust since the Precambrian. *Nature* **497,** 367–360 (2013).
38. Burow, K. R., Nolan, B. T., Rupert, M. G. & Dubrovsky, N. M. Nitrate in groundwater of the United States, 1991–2003. *Environ. Sci. Technol.* **44,** 4988–4997 (2010).
39. Graham, J. P. & Polizzotto, M. L. Pit latrines and their impacts on groundwater quality: a systematic review. *Environ. Health Perspect.* **121,** 521–530 (2013).
40. Sorensen, J. P. R. *et al*. Emerging contaminants in urban groundwater sources in Africa. *Water Res.* **72,** 51–63 (2015).
41. MacDonald, A. M. *et al*. Groundwater quality and depletion in the Indo-Gangetic Basin mapped from *in situ* observations. *Nat. Geosci.* **9,** 762–766 (2016).

Acknowledgements

S.J. was supported by an NSERC Discovery Grant. R.G.T. acknowledges support of the NERC-ESRC-DFID UPGro grant NE/M008932/1.

Author contributions

S.J. and J.W.K. analysed the compiled groundwater isotope data and wrote initial drafts of the manuscript. S.J. and D.P. analysed the compiled groundwater well construction data. All authors discussed results and edited the manuscript.

Additional information

Supplementary information is available in the online version of the paper. Reprints and permissions information is available online at www.nature.com/reprints. Publisher's note: Springer Nature remains neutral with regard to jurisdictional claims in published maps and institutional affiliations. Correspondence and requests for materials should be addressed to S.J.

Competing financial interests

The authors declare no competing financial interests.

Methods

Global groundwater isotope data. We analysed global groundwater isotope data compiled from hundreds of primary literature sources and from the United States Geological Survey's Water Quality Portal (Supplementary Tables 1 and 2). About two-thirds (65%) of our global radiocarbon compilation comes from North America, which represents only ~18% of global ice-free lands. By contrast, only 9% and 11% of our compiled radiocarbon data come from Africa and Asia, which each comprise much larger shares of the global landmass (~22% and ~33% of global ice-free lands, respectively; Supplementary Fig. 2). We analysed the compiled groundwater isotope data to partition the fraction of groundwater samples that recharged before the Holocene–Pleistocene transition 11,700 years ago ('fossil groundwater', based on ^{14}C with a half-life of 5,730 years), and more recently than 1953, when the 'hydrogen bomb peak' in meteoric tritium began ('post-1953 groundwater', based on ^{3}H with a half-life of 12.3 years).

Determining fossil groundwater fractions. We used stable ($\delta^{13}C$) and radioactive (^{14}C) carbon isotope data to calculate fossil groundwater fractions (F_{fossil}) following (ref. 20):

$$F_{Fossil} = 1 - \frac{^{14}C_{sample} - {}^{14}C_{fossil}}{^{14}C_{Holocene} - {}^{14}C_{fossil}} \quad (1)$$

where dissolved inorganic carbon concentrations are assumed to be roughly equal for the fossil and Holocene waters[20], and ^{14}C represents the radiocarbon activity of: the groundwater sample (subscript 'sample'), Holocene groundwater recharged within the past 11,700 years (subscript 'Holocene'), or fossil groundwater recharged more than 11,700 years ago (subscript 'fossil'). Holocene and fossil ^{14}C inputs are based on late-Quaternary atmospheric ^{14}C time series[42,43] corrected for radioactive decay following (ref. 20):

$$^{14}C_t = \left(q_t \, {}^{14}C_{precip(t)} e^{-0.693(t_{sample}-t)/(5{,}730\,years)} \right)_t \quad (2)$$

where $^{14}C_{precip(t)}$ represents precipitation ^{14}C at time t, and t_{sample} is the date that the groundwater sample was analysed. $^{14}C_{Holocene}$ is represented by $^{14}C_t$ evaluated for the time interval of $0 < abs(t_{sample} - t) < 11{,}700$ years; $^{14}C_{fossil}$ is represented by $^{14}C_t$ evaluated prior to the Holocene (that is, $abs(t_{sample} - t) > 11{,}700$ years). For years postdating thermonuclear-bomb testing, we apply a 10-year running average to estimate the maximum possible $^{14}C_{Holocene}$ value (Supplementary Fig. 5), effectively assuming some amount of dispersion has taken place in most aquifer systems over the past 50 years. The factor q is used to correct for the dissolution of carbonate with zero radiocarbon:

$$q_t = \frac{\delta^{13}C_t - \delta^{13}C_{carbonate}}{\delta^{13}C_{recharge} - \delta^{13}C_{carbonate}} \quad (3)$$

where $\delta^{13}C_{recharge}$ and $\delta^{13}C_{carbonate}$ are the stable isotope compositions of recharge and carbonates. We used $\delta^{13}C_{recharge}$ and $\delta^{13}C_{carbonate}$ values reported in the compiled studies when available, and otherwise assumed[20] $\delta^{13}C_{carbonate} = 0‰$ and $\delta^{13}C_{recharge} = -14.3‰$ PDB (Pee Dee Belemnite). Global $\delta^{13}C_{carbonate}$ and $\delta^{13}C_{recharge}$ values vary around the globe[20] such that our assumption of $\delta^{13}C_{carbonate} = 0‰$ and $\delta^{13}C_{recharge} = -14.3‰$ introduces uncertainty into our fossil groundwater calculations.

The range of $\delta^{13}C$ values ascribed to each time interval ($\delta^{13}C_t$) is assumed to be constrained by $\delta^{13}C_{recharge} \le \delta^{13}C_{Holocene} \le \delta^{13}C_{sample} \le \delta^{13}C_{fossil} \le \delta^{13}C_{carbonate}$ (ref. 20). Because the possible ages of the Holocene and pre-Holocene endmembers vary widely, the ranges of $^{14}C_{Holocene}$ and $^{14}C_{fossil}$ values are often large; we apply upper and lower limits of $^{14}C_{Holocene}$ and $^{14}C_{fossil}$ in equation (1) to estimate minimum and maximum fossil groundwater fractions. $^{14}C_{Holocene}$ and $^{14}C_{fossil}$ share an identical endmember at the 11,700-year boundary. The shared 11,700-year endmember, and the large atmospheric radiocarbon variations over each endmember interval, lead to highly uncertain F_{fossil} calculations for some samples.

In each aquifer, we pinpointed two depths where we observed transitions from Holocene groundwater to pre-Holocene fossil groundwater, and used these depths as upper and lower limits in the bar graphs shown in Fig. 1. The first (shallower) recorded transition depth specifies a depth below which the majority (>50%) of well water samples from a given aquifer must contain some fraction of fossil groundwater (that is, over half the samples have a minimum fossil groundwater fraction of greater than zero). The second (deeper) recorded transition depth represents a depth below which the majority (>50%) of sampled well waters from a given aquifer system contain mostly fossil groundwater (that is, over half of the samples deeper than the depth have a minimum fossil groundwater fraction exceeding 50%).

Where oxygen stable isotope data are also available, we confirmed the depth to fossil groundwater by comparing the $^{18}O/^{16}O$ ratio in groundwater to a new global map of $\delta^{18}O$ in late-Pleistocene precipitation[44]; where $\delta^{18}O = ([^{18}O/^{16}O_{sample}]/[^{18}O/^{16}O_{standard\ ocean\ water}] - 1) \times 10^3‰$. Late-Holocene and late-Pleistocene precipitation $\delta^{18}O$ values are detectably different (>1‰) over the great majority (~87%) of the global landmass[44], enabling use of depth-$\delta^{18}O$ plots as a qualitative secondary indicator of the depth to fossil groundwater.

Determining post-1953 groundwater fractions. To calculate the fraction of modern, post-1953 groundwater in a sample we used globally interpolated precipitation tritium for years spanning the pre-bomb era (prior to 1950) to 2010 from ref. 24. Global precipitation ^{3}H estimates derive from >60,000 monthly ^{3}H measurements made at 738 globally distributed stations (data provided by the International Atomic Energy Agency: iaea.org/water). We then weighted the monthly precipitation ^{3}H data against the long-term average monthly precipitation rate[45] to estimate an annually integrated precipitation ^{3}H value at each well site. Once a precipitation tritium record was developed for each well location (from ref. 24), we decay-corrected the precipitation tritium input curve to the date that each sample was collected[20]. As in our radiocarbon-based calculation, we assume that some amount of dispersion takes place in the aquifer and apply a 10-year running average before calculating maximum and minimum possible $^{3}H_{post-1953}$ values (Supplementary Fig. 5). We then applied the range of possible decay-corrected, post-1953 precipitation ^{3}H values as one endmember in a two-component mixing model, and pre-1953 precipitation ^{3}H as the other component:

$$F_{post-1953} = \frac{^{3}H_{sample} - {}^{3}H_{pre-1953}}{^{3}H_{post-1953} - {}^{3}H_{pre-1953}} \quad (4)$$

where $^{3}H_{sample}$ is the measured ^{3}H in the groundwater sample, and $^{3}H_{pre-1953}$ and $^{3}H_{post-1953}$ are the local meteoric water tritium activities that have been decay-corrected to the time of sampling for either prior to 1953 ($^{3}H_{pre-1953}$), or years after 1953 ($^{3}H_{post-1953}$). The year 1953 was selected as a threshold[20] so that the overwhelming majority of possible $^{3}H_{pre-1953}$ values fall below analytical detection limits, leading us to assume $^{3}H_{pre-1953} \approx 0$. We assume subterranean tritium production leads to secular equilibrium tritium contents that do not exceed the common analytical detection limit of 0.8 tritium units.

Estimating groundwater age-storage volumes. In Fig. 2 of the main text, we present ranges of fossil and post-1953 groundwater with depth. The ranges shown represent averages of the minimum and maximum fossil groundwater (or post-1953 groundwater) fractions at each depth interval. For example, the range of fossil groundwater from 0 m to 25 m depth shown in Fig. 2a is 3%–52%, where 3% is the average minimum fossil groundwater fractions among all $n = 627$ wells perforated in the uppermost 25 m of the crust, and 52% is the average maximum fossil groundwater fraction for these $n = 627$ well waters.

Data availability. Compiled groundwater isotope data are available in the primary references listed in Supplementary Tables 1 and 2 and in tabulated form in the Supplementary Information. Additional groundwater isotope data for the USA used in this analysis can be downloaded from https://www.waterqualitydata.us.

References

42. Reimer, P. J. *et al*. IntCal13 and Marine13 radiocarbon age calibration curves 0–50,000 years cal BP. *Radiocarbon* **55,** 1869–1887 (2013).
43. Hua, Q. & Barbetti, M. Review of tropospheric bomb ^{14}C data for carbon cycle modeling and age calibration purposes. *Radiocarbon* **46,** 1273–1298 (2004).
44. Jasechko, S. Late-Pleistocene precipitation $\delta^{18}O$ interpolated across the global landmass. *Geochem. Geophys. Geosyst.* **17,** 3274–3288 (2016).
45. New, M., Lister, D., Hulme, M. & Makin, I. A high-resolution data set of surface climate over global land areas. *Clim. Res.* **21,** 1–25 (2002).